Seventh International Conference on CFD in the Minerals and Process Industries
CSIRO, Melbourne, Australia
9-11 December 2009

COMPUTATIONAL FLUID DYNAMICS IN THE PULP AND PAPER INDUSTRY - THE DESIGN OF A HIGH PERFORMANCE PULP SCREEN ROTOR

James A. Olson, Sean Delfel, Carl Ollivier-Gooch and Robert W. Gooding*

Pulp and Paper Centre, Department of Mechanical Engineering,
University of British Columbia, Vancouver CANADA

*Advanced Fibre Technologies Inc., Montreal CANADA

ABSTRACT

The pulp and paper industry has a large number of diverse unit operations. Many of these unit operations are modelled using Computational Fluid Dynamic (CFD) simulations to provide a better understanding of the underlying physics, to develop high performance equipment and to design advanced control systems. The application of CFD to fibre suspension flows and processing is challenging due to the complex rheology of the fibre suspension and the wide range of mass concentrations, fibre properties and shear rates employed by the various operations in the process. Due to the complexity and the varying model requirements a range of models are used. A brief review of pulp suspension rheology, the methods used to model this complex suspension and some industrial applications are given.

The application of CFD to the development of a high performance pulp screen rotor is given in detail. A CFD simulation was developed and used to design a novel Multi-Element Foil rotor. The simulations are validated against laboratory and pilot experiments. Based on the CFD optimization, an industrial prototype was developed and tested in an industrial pressure screen in a Newsprint recycle mill. The new rotor was shown to provide a 43% energy reduction over the state of the art rotor technology.

INTRODUCTION

Pulp and paper manufacture is a global, large scale and complex industry that produces the world's most widely used ubiquitous commodities. The pulp and paper industry includes the conversion of natural wood material, typically wood chips or recycled material, into paper used for printing and writing, packaging and hygiene products.

The natural cells that form trees are long thin, hollow fibres made of cellulose and hemicelluloses that are held together by lignin, a thermal plastic polymer. The cells or fibres are approximately 3mm long in softwoods and 1 mm long in hardwoods. Both have an aspect ratio of approximately 100. Separated fibre suspensions are called pulps.

Pulping is the process of separating the individual fibres from the wood [Sixta 2006]. There are essentially two methods of pulping: Mechanical pulping where wood chips are passed between large metal discs with bars and grooves that shred the wood into individual fibres and Chemical pulping where the lignin polymer that holds the cellulose fibres together is dissolved in a solution of NaOH and Na_2S (pulping liquor), releasing the nearly pure cellulose fibres, largely intact. The fibres are subsequently washed, screened, bleached and the water removed for transport. The dissolved lignin and hemi-cellulose suspension is burned to create power and heat. The smelt containing Na and S is then recovered through a multistep recovery process for reuse.

Recycling is the process of separating the fibres from paper material and removing contaminants from the fibre suspension so that the fibres can be reformed into paper. The reclaimed paper or corrugated containers are combined with water into large repulpers that provide high shear and agitation until the fibres are separated. The suspension than passes through a number of unit operations designed to remove a wide range of contaminants and inks. These processes include screens, hydrocyclones, flotation cells, etc.

Papermaking is the conversion of a dilute pulp suspension into a paper sheet through three essential processes: forming, pressing and drying. In forming, the1% by mass suspension travels through a turbulence generating tube bank then a linear contracting duct to create a planar jet approximately 1 cm thick by 10 m wide moving at more than 20 m/s. The jet impinges between two moving filters where most of the water is removed from the pulp through a combination of suction and pressure caused by wire tension. After forming the suspension in nearly 20% solids. The suspension is further concentrated to nearly 40% solids by pressing between two or more rotating cylinders and the final moisture is removed through drying by passing the suspension over a large number steam heated metal cylinders. The resulting dried paper rolled and shipped to printers and converters.

Computational fluid dynamics (CFD) has been an integral tool for the development and optimization of the entire industry. However, there are significant challenges for CFD practitioners who model the fibre suspension flow. The pulp is a natural poly-disperse fibre suspension with a large variation of fibre lengths and aspect ratios. The process contains a large number of unique unit operations that have complex, multi-scale flow characteristics and these operations require a wide range of suspension concentrations from the extreme dilute to nearly solid.

FIBRE SUSPENSION RHEOLOGY AND CFD MODELING

To understand some of the difficulties of applying CFD to the pulp and paper industry, a brief review of the fibre suspension rheology is required. Fortunately, there exists a number of excellent reviews of pulp fibre suspension properties that provide a detailed analysis of the wide range of flow and concentration regimes and the associated literature [e.g., Kerekes 2006; Cui and Grace 2007; Soderberg and Norman 2001] and the reader is directed to these for more detailed reviews.

The suspension rheology is strongly affected by the concentration and physical properties of the fibre particles. Wood fibres have a broad range of lengths that is determined by both natural variation and the degree of cutting that they may experience during processing. The fibres are also flexible and can be deformed during processing, both from hydrodynamic shear and from physical interactions with equipment and each other. The deformations result in a suspension of curled and kinked fibres. The flexibility of the fibres depends on the cross sectional shape and the elastic modulus of the fibre material which is also dependent on natural variation and processing. For example, chemical pulping produces long, uncut fibres that can be very flexible, whereas, mechanical pulps produce short, stiffer fibres.

During processing in the various unit operations, the suspension exists over a wide range of concentrations and shear rates. The mass concentration can range from 0.01% in effluent treatments, to near 1% during papermaking and hydrocyclone operations, to 2-4% for screening operations, to 10% for storage and bleaching operations, to 20% for chemical pulping to 40% during pressing up to 90% for drying operations. The rheology changes significantly over this concentration range.

The flow regimes for pulp are characterized by the dimensionless fibre concentration and shear rate. The dimensionless concentration is given by the volume of fibres normalized by the volume of a sphere swept out by the average fibre length. This can be expressed as

$$N = \frac{2C_v}{3}\left(\frac{L}{d}\right)^2$$

where N is the average number of fibres in the sphere, L is average fibre length, d is average fibre diameter and C_v is the volume concentration of fibres. N is often referred to as the Crowding factor in pulp and paper literature [Kerekes and Schell 1992].

For N << 1 the suspension is considered to be dilute and the fibres are non-interacting. The rheology is essentially that of water and there exists only one-way coupling between the fibre and fluid phases. However, for some applications the orientation of fibres is important, for example, the fibre orientation distribution during forming can determine the strength and the strength isotropy of the resulting paper.

In this regime, fibre orientation has been modelled in both turbulent and laminar flows. The flow of slender bodies in dilute laminar flow is the subject of many researchers, e.g., Jeffrey (1922), Bretherton (1962), and Cox (1970). However, there are far fewer that examine the motion of fibres in turbulent flow (e.g. Olson and Kerekes, 1998 and Olson et al, 2004).

As N approaches 1, the number of fibre interactions increases and the suspension is considered semi-dilute and fibres begin to interact hydrodynamically. The effects of these hydrodynamic interactions on the fibre orientation distribution of the suspension are modelled assuming that interactions are random perturbations to the fibre orientation. From this assumption, the effect can be modelled as a diffusion process where the rotational diffusion coefficient is typically given as linearly proportional to the strain rate [Doi and Edwards 1984 Folgar and Tucker 1984, Koch 1995, Krochak 2009]. A similar approach has been used to model the orientation distribution of fibres in turbulent flow where the fibre orientation perturbations come from the random fluctuations of the turbulent fluid. The application of a rotary diffusion coefficient has been successfully used to model the final orientation state leaving the papermachine headbox [Olson et al, 2004, Hyensjo et al 2007] during papermaking.

Fibre concentration and orientation also affects the fluid flow, that is, the fluid phase is coupled to the fibre phase. To model the coupling between phases, the stress imposed on the fluid by the fibres needs to be modelled. Analytic and experimental results, have shown that the fibre stress is a complex function of concentration, strain rate and fibre orientation distribution [e.g., Hämäläinen et al 2008, Krochak et al 2009].

As N increases beyond 1, fibres begin to collide and interact through mechanical contact. At N approximately 16 the fibres span the suspension and form a load-bearing network (the gel point) that significantly affects the rheology of the suspension [Martinez et al 2001]. As N increases, the strength of the fibre network continues to increase. At N>60, the fibres are thought to be in continuous mechanical contact. The existence of this fibre network within the suspension manifests itself in several ways which needs to be considered when developing a pulp suspension CFD model.

First, the suspensions exhibits a yield stress and is shear thinning [Bennington 1990, Wikstrom and Ramusen 1998]. Recent work by Gomez [2009] summarizes and extends some of the rheological characterization nicely. In her work, she showed that the yield stress is related to the mass concentration by the following correlations (which agree with previous measurements):

$\tau_y = 12.3{C_m}^{2.05}$ for softwood pulp

$\tau_y = 1.25{C_m}^{3.00}$ for hardwood pulp

Further, she showed that the laminar pulp suspension could be reasonably modeled as a Herschel-Bulkley fluid, given by

$$\tau = \tau_y + \dot{\gamma}^n$$

where τ_y is given by the previous correlation and n is approximately -0.28+/-0.05 for pulps in the range of 0.75 wt.% to 2.5wt%. As an example, Figure 1 shows the shear stress – strain rate relationship for a fully bleached softwood kraft (FBK) pulp suspension over a range of mass concentrations [Gomez, 1999].

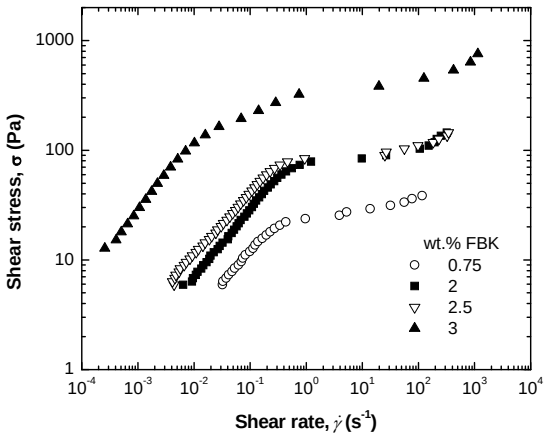

Figure 1: The shear stress – strain rate relationship for Fully Bleached Softwood Kraft pulp [Gomez 1999].

To model the complex flow in an industrial pulp mixing chest the above Herschel-Bulkley fluid model and the experimentally measured correlations for mass concentration, were implemented into a CFD simulation. The presence of the fluids yield stress creates a "cavern" or yield surface in the mixing chest. Ensuring adequate mixing requires the entire fluid has yielded. The size of the cavern is known to correlate with the momentum induced by the impeller which is a function of speed (and power) and design. An example, of the cavern size for three impeller rotational numbers (powers) is shown in Figure 2 [Gomez 2009]. In this work, the performance of laboratory and industrial pulp mixing systems were modelled and compared with experimental measurements to validate the CFD approach and to assess the effectiveness of the different impeller and chest designs.

Figure 2 shows the yield surface for 3 impeller rotor speeds in an industrial pulp mixing chest.

Second, for N>16 the fibre network is able to support its own pressure. In this region, the fibre phase and the fluid phase are often modelled using a two-phase flow model where the fibre phase undergoes compression and motion and the fluid phase passes through the fibre network. In such two-phase modelling, the inter-phase momentum transfer is typically modelled using flow-pressure relations (Ergun equations) from the flow through porous media where the resistance of the porous media depends on the compressibility and porosity of the fibre phase. A recent implementation of this type of model, along with reaction kinetics and temperature, is given by Pougatch, Salcudean and Gartshore (2006) where they modelled the flow of pulping liquor (liquid phase) and the fibre phase in a continuous chemical pulping vessel (digester) where fibres and the reacting liquid enter the top and move downward and out the bottom. Figure 3 below shows examples of the fibre mass fraction and the compression of the fibre network as they move within this vessel. Note that the fibres at the bottom of the reaction vessel are significantly more compressed than at the top. The Figure shows the pulping fluid velocity vectors in the vessel. The recirculation zones where the liquor is extracted and added to the suspension is evident.

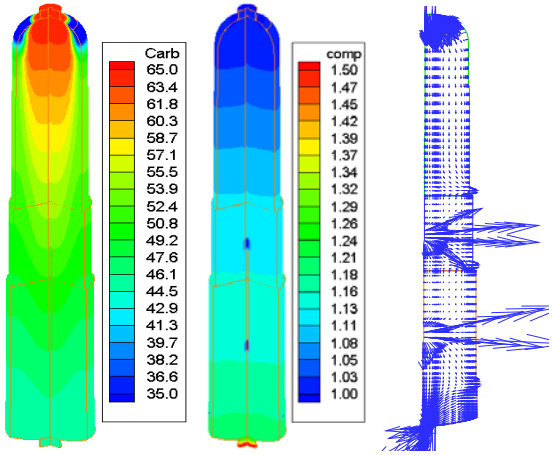

Figure 3: A two phase CFD model of the fibre/carbohydrate mass fraction (left), the fibre phase compression (middle) and the liquid phase velocity vectors (right).

Third, the network forms non-uniform concentrationds of fibers called flocs. The mechanism of floc formation has been outlined by Mason [1948] but they are essentially bundles of fibres that have been brought together by fluid forces and become mechanically held by fibre-fibre friction, for example see Figure 4. The details of the mechanism of floc formation are still a subject of ongoing research. These mass concentrations are frozen into the paper during papermaking and reduce the paper strength, optical and printing quality. Although formed by hydrodynamic forces that bring the fibres together, the flocs can also be separated through shear and elongation and are therefore transient. This transient creation and destruction of flocs by the flow conditions has been modelled using CFD to predict the mass distribution in the resulting paper sheet [e.g., Hammaleinen et al 2008].

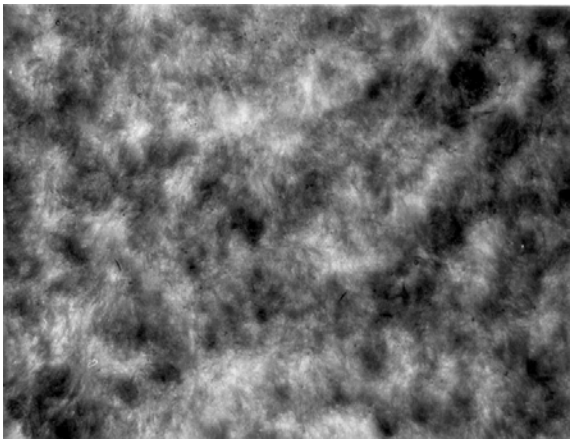

Figure 4: Photo of flocculated suspension of fibres showing the variation of mass distribution [from Kerekes 2009]. Mass concentration 0.5% N=76 softwood kraft pulp (fir).

For turbulent flow conditions, where the network is completely fluidized and for concentrations in the range of 1 to 5 wt.% (N>1), the suspension experiences turbulent drag reduction [Kerekes and Douglas 1972] which is a significant reduction in the wall shear stress of the suspension over that of just water.

APPLICATIONS TO PULP SCREEN ROTOR DESIGN

Despite the complexity of the pulp suspension rheology, CFD has been successfully used to design significantly improved pulping and pulp processing systems. In recent work, we have used CFD to design and optimize a high performance pulp screen rotor to significantly reduce the energy requirements of this unit operation. Although the model does not capture all of the suspension rheology, CFD has been a useful tool to designers of such equipment.

In applications to pressure screening the suspension is typically 1-3 wt % solids and under extreme turbulent shear. In this regime, the fluid is expected to have turbulent drag reduction properties and indeed the screen operators know that a screen full of water has a higher power draw than when filled with pulp. Turbulent drag reduction may also affect the separation and stall characteristics of the fluid but this is speculation. In this work, we simplify the model by assuming a Newtonian fluid but recognize that the model will not capture the correct power.

Pressure screens are the most industrially effective method of removing oversize contaminants, such as, stickies and shives that reduce the strength, smoothness and optical properties of paper. During screening the pulp suspension is passed through narrow slotted apertures in a cylinder to remove oversized debris from the pulp stream. The slots are approximately 0.15 mm wide and the fibres can be 3 mm in length. As a result, the apertures become quickly plugged with fibres and prevent the suspension from passing through the screen cylinder. To prevent screen plugging, hydrodynamic foils attached to a rotor are passed over the screen apertures to create a negative pressure pulse and backflush the apertures, clearing them of pulp accumulations and maintaining flow through the screen.

The faster the rotor rotates the stronger the negative pressure pulse and the higher the maximum possible flow rate through the screen. However, the power required by the rotor increases with rotor tip speed, V_t, to the third power [Olson et al 2004] and small changes in speed can make large changes in the energy required and total operating cost. Therefore, an optimal rotor design would create a high negative pressure pulse to maintain flow while operating at the lowest possible speed.

Previous experimental and computational studies have examined the effect of rotor design on screen performance [Feng et al 2005]. Increasing the camber (i.e. the curvature) of the foil was also shown to increase the strength and width of the negative pressure pulse generated by the rotor. The high camber foils where found, however, to stall almost immediately at a very small angle-of-attack. In order to obtain the effect of a highly cambered foil at a high angle-of-attack, multi-element foil (MEF) technology was developed for a pulp screen [Delfel et al 2008]. Similar to the flaps on an aircraft deployed during landing, multi-element airfoils generate high lift (negative pressure) at low speeds enabling high camber foils to operate at positive angle-of-attacks without stalling. Stall is prevented by allowing higher energy fluid from the lower surface of the foil to pass through the slot between the main foil and the flap in order to re-energize the boundary layer on the upper surface of the foil.

To determine the optimal design configuration of a multi-element foil rotor a systematic computational fluid dynamic simulation study was completed [Delfel et al 2008]. The angle-of-attack, flap angle and position were optimized for our multi-element foil rotor. In this study, FLUENT 6.1 was used to numerically solve the discretized Navier-Stokes equations. The problem was assumed to be two dimensional, and steady state, allowing the Navier-Stokes equations can be reduced to the continuity and x- and y-momentum equations. Turbulence was modelled using the standard k-ε turbulence model with enhanced wall treatment. The solver is a second-order finite volume solver: control volume averages are found for each flow variable and the fluxes at the control volume faces are then found through a second-order spatial interpolation from the control volume centre.

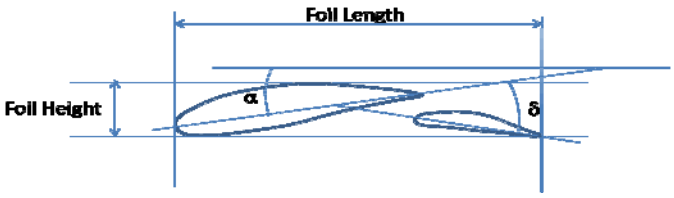

Figure 5: MEF showing angle-of-attack, α, and flap angle, δ.

The effect of varying flap angle, α, can be seen in Figure 6, that shows pressure contours and streamlines for a multi-element foil at varying flap angles with a constant angle-of-attack of $\alpha = -8.83$ *deg.* As can be seen, deflecting the flap, which is effectively an increase in the

camber of the foil, causes the pressure pulse to widen and strengthen until δ = *27.83 deg.*, after which the flow over the flap begins to separate and suction at the wall diminishes. At δ = *44.83 deg.*, the flap has stalled fully and the beginnings of vortex shedding can be seen. Interestingly, increasing flap angle also has the affect of forcing the stagnation point towards the lower surface of the leading edge of the foil, diminishing the positive pulse on the screen. It is thought that the presence of a strong positive pulse results in debris being pushed through the apertures and a reduction of debris removal efficiency.

Similarly, the effect of angle-of-attack, α, was determined [Delfel 2009]. From the α- and δ-sweep data was combined to make surfaces of the minimum pressure on the cylinder (Suction pulse magnitude) given in terms of non-dimension pressure, C_P, where

$$C_p = \frac{P}{1/2\,\rho V_t^2}$$

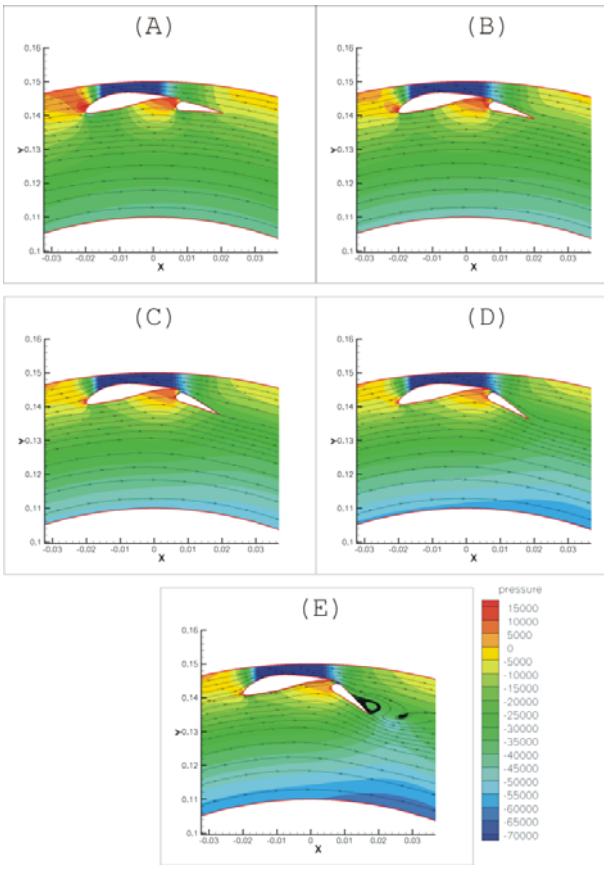

Figure 6: Pressure contours and streamlines for a multi-element foil at (A) δ = 15.8 deg., (B) δ = 23.8 deg., (C) δ = 30.83 deg., (D) δ = 37.8 deg., and (E) δ = 44.8 deg. The foil is at α = -8.8 deg. for all cases. [Delfel 2009]

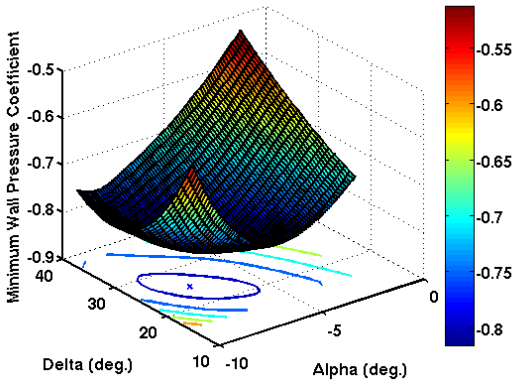

Figure 7: Surfaces of minimum wall pressure coefficient vs. foil angle-of-attack and flap angle showing the optimal configuration [Delfel 2009].

The C_P values, versus both α and δ, are shown in Figure 7. Minimum C_P is shown to have a strong dependence on flap angle for angles-of-attack at which the flow is fully attached, creating a clear minimum of C_P = *-0.82* at (α, δ) = *(-7.63, 24.83)*. Beyond α =*-1.83 deg.*, any deflection of the flap causes the foil to stall and the pressure becomes independent of flap angle.

Pilot screening trials

To experimentally validate the fluid and pressure simulations and to determine the performance of the optimal multi-element foil rotor a series of pilot screening trials were conducted for a range of angle-of-attack and flap angle configurations [Hamelin, 2009].

The study was conducted at the FPInnovations – Paprican Division, Vancouver screening pilot plant using an instrumented Hooper PSV 2100 pressure screen [Hamelin et al, 2009]. The screen was equipped with a variable frequency drive (VFD), allowing for rotor tip speeds of up to 20 m/s. A wedge-wire cylinder with a 3.2 mm wire width, 0.9 mm contour height, and a 0.2 mm slot width was used in the trial. The cylinder has a diameter of 0.286 m and an open area of 5.98%. Due to the large diameter bearing column on the lower half of the screen, the cylinder was modified by covering the lower 9 out of 15 rings with metal strips, reducing the active screening area and allowing the use of a shorter foil length, appropriate for the bearing housing. The effective open area of the screen after the modifications was 8.7×10^{-3} m^2.

The pulp used was a 1.5% consistency 50% hardwood, 50% softwood (by mass) kraft pulp which represents a model deink pulp. The feed was supplied from a 10,000 L stock tank kept at a nominal temperature of 49° C. Feed samples were collected at least once for each rotor configuration, while reject and accept samples were collected at a slot velocity of 1.0 m/s for every rotor speed.

For each rotor configuration tested the maximum slot velocity-power curve was determined by setting the rotor speed to a constant value and increasing the slot velocity (fluid velocity through the screen slots, V_s) until the onset of plugging. The point of maximum slot velocity versus rotor power, creates a failure envelope (or maximum slot velocity envelope) for each rotor and is used to compare the performance of each configuration.

Figure 8: Photograph of prototype adjustable MEF rotor used in the pilot trials showing the slot between main foil and flap.

The angle-of-attack, α, is the angle of the main foil chord with respect to the horizontal, and the flap angle δ is the angle between the flap chord and the main foil chord. Three different angles-of-attack were tested, varying from -8.83 deg. to -3.33 deg., and at each angle-of-attack three separate flap angles were tested, varying from 18.83 deg. to 28.83 deg. In addition to the MEF foil rotor configurations, an optimized single foil rotor EP was tested for comparison.

The maximum capacity envelopes for the two best MEF and EP rotors are shown in Figure 9. The key gains in performance for the MEF come from its ability to run reliably below a tip speed of 10 m/s. Several of the MEF configurations ran reliably at 8 m/s, and the suboptimal MEF configurations performed similarly to the EP. Configuration 3, corresponding to α=-3.33 deg and δ=23.83 deg, had the lowest minimum power consumption measured: 2.0 kW at V_t = 8.0 m/s, V_s = 2.68 m/s, a 26% reduction in minimum power versus the single foil, EP. Configuration 6, corresponding to α=-3.33 deg and δ=18.83 deg, had the highest capacity at a given rotor power, with an improvement of 31% in maximum slot velocity versus the single foil (EP) at V_t = 12 m/s and a constant power of approximately 3 kW.

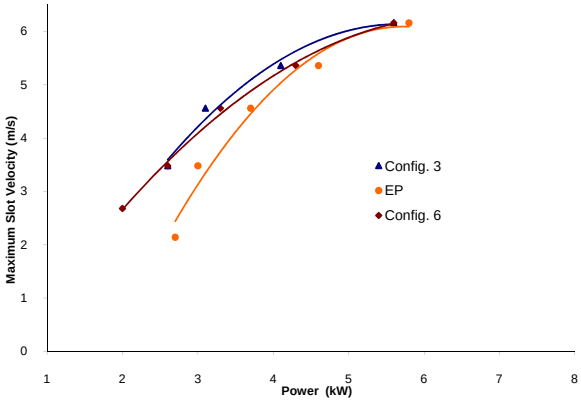

Figure 9: Plugging envelopes for the two best MEF rotors and the EP (single foil) rotor [Hammelin et al 2009].

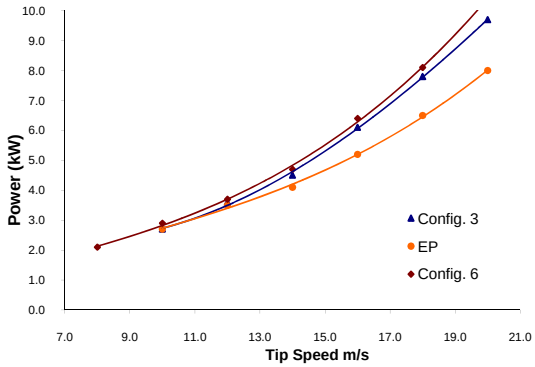

Figure 10: Effect of tip speed on rotor power consumption at V_s=1.0 m/s.

Figure 10 shows power consumption as a function of rotor tip speed. As expected, since single-element foils typically have lower drag coefficients, the EP rotor uses less power at a given tip speed than the MEF. The power savings for the MEF come from its ability to operate at lower tip speeds.

Mill Prototype Testing

A prototype MEF rotor was installed in a Black Clawson UV 300 at a recycle de-ink mill (See Figure 8). The screen was equipped with a 0.12 mm (0.005") narrow slotted MacroFlow™ MF0623 screen cylinder. A parallel screen was originally equipped with a Black Clawson 4-foil and 2-foil rotor and a 0.15mm (0.006") slotted screen cylinder. The rotor and cylinder were later replaced with an AFT EP™ rotor and 0.12 mm (0.005") slotted screen cylinder. This enabled the performance of the four rotor-cylinder combinations to be compared.

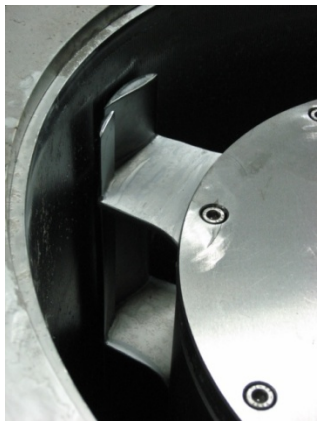

Figure 11: A photograph of the installed prototype AFT MEF™ Rotor. The main foil and flap can be seen next to a screen cylinder.

The rotor tip speed was varied using AFT's variable frequency drive (VFD) which was brought to the mill and installed on the MEF trial screen. Figure 12 shows the power versus tip speed for the AFT MEF™ rotor and the other rotors at 20.8 m/s. The MEF™ rotor was initially installed and ran at 20.8 m/s. At this speed it consumed less power than the Black Clawson 4 foil rotor (66.3HP) and the EP™ rotor (73.3 HP). The Black Clawson 2 foil rotor consumed 57.4HP at a tip speed of 20.8 m/s.

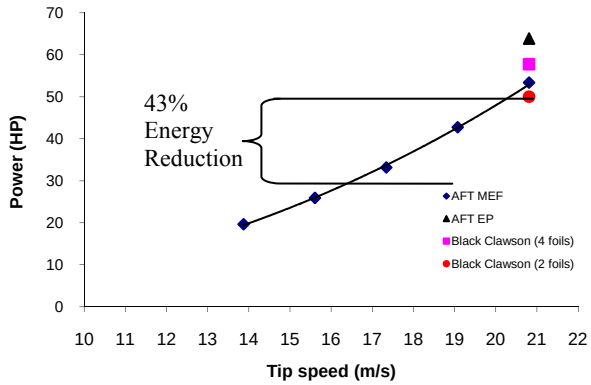

Figure 12: Power versus tip speed for the AFT MEF™ Rotor, EP™ Rotor and the Black Clawson 4 foil and 2 foil rotors. The MEF™ rotor provides a 43% energy reduction over the Black Clawson and Single Element EP foil rotor.

To determine the minimum power required to maintain capacity using the AFT MEF™ rotor the VFD was used to decrease rotor speed in 1.7 m/s increments. When the rotor was reduced to 13.9 m/s it began to plug over time. The rotor speed was then increased to 17.3 m/s to ensure adequate capacity. At this conservative rotor speed, the resulting energy savings over the Single foil rotor is approximately 43%. The rotor speed could have most likely been reduced to 15.6 m/s which would have resulted in an energy savings of 61%.

CONCLUSIONS

The pulp and paper industry has a wide range of unit operations with many applications for Computational Fluid Dynamics, from generalized industrial systems, such as, boilers, kilns, turbines, effluent treatments systems, etc. to specialized pulp and paper systems, for example, screens, cleaners, headboxes, presses, etc. In addition, there is renewed interest in modelling and optimization with the push for energy efficiency and increased production.

Application of CFD to the pulp and paper industry, especially to model pulp suspension flows, is complex. The high aspect ratio pulp fibres are orientable, interact over long range hydrodynamic forces, interact through mechanical entanglement to form a load bearing networks and transient fibre flocs, and under conditions of high turbulence where the suspension is fully fluidized, exhibit the unusual property of reducing the turbulent drag of the suspension. The models that are developed are specific to the problem of interest and often require simplifications. However, despite these challenges, CFD has still been an extremely useful tool not only for researchers but to equipment and process design engineers.

In the specific application to pulp screening equipment design, a CFD simulation was used to design and optimize a novel Multi-Element Foil rotor. The simulations coupled with experimental validation enabled the design and construction of an industrial prototype that could be tested in a de-ink newsprint mill. The prototype MEF rotor was shown to provide a 43% energy reduction with no significant change in operating ability over the conventional state-of-the-art single element foil rotor.

ACKNOWLEDGEMENT

The author would like to thank AFT Inc. and BC Hydro - Power Smart for their strong support of this research and FPInnovations-Paprican Division for the donation of the pilot screening facility where all the pilot trials were run. I also acknowledge the financial support of NSERC.

REFERENCES

BENNINGTON, C.P.J., KEREKES, R.J. AND GRACE, J.R., (1990). The yield stress of fibre suspensions, Can. J. Chem. Eng. 68, 10, 748−757.

BRETHERTON, F.P. (1962) The Motion of Rigid Particles in a Shear Flow at Low Reynolds Number J. Fluid Mech. 14, 284.

COX, R.G. (1970) The Motion of Long Slender Bodies in a Viscous Fluid J. Fluid Mech. 44, 791–810.

CUI H., GRACE J., (2007) "Flow of pulp fibre suspension and slurries: A review" International Journal of Multiphase Flow, 33 921–934.

DELFEL, S., OLLIVIER-GOOCH, C. AND OLSON, J.A. "A numerical investigation into the effectiveness of multi-element pressure screen rotor foils", ASME-J. Fluids Eng., *in press*, 2008

DOI, M. & EDWARDS, S.F. (1984) "The Theory of Polymer Dynamics" Oxford University
Press New York.

FENG, M., GONZALEZ J., OLSON, J.A., OLLIVIER-GOOCH, C., AND GOODING, R.W., (2005). "Numerical simulation of the pressure pulses produced by a pressure screen foil rotor", J. Fluid Eng. 127(2):347-357.

FOLGAR, F. & TUCKER, C.L. (1984) Orientation Behavior of Fibres in Concentrated Suspensions *J. Reinf. Plastics and Comp.* **3** 98–119.

GOMEZ C., (2009) "Numericl and experimental investigation of macro-scale mixing applied to pulp fibre suspensions", PhD Thesis, University of British Columbia.

HÄMÄLÄINEN J., (2008) "Prediction of the Sheet Formation Using the Fibre Floc Evolution Model", PaperCon '08, TAPPI/PIMA/Coating Conference, & Trade Fair, Dallas, Texas, USA.

HÄMÄLÄINEN J., HÄMÄLÄINEN T., MADETOJA E., RUOTSALAINEN H., (2008) CFD-based Optimization for a Complete Industrial Process: Papermaking, in "Optimization based on Computational Fluid Dynamics", Ed. by D. Thevenin, Springer,

HAMELIN[1] M., DELFEL S., OLSON J., OLLIVIER-GOOCH C.F. (2009), High Performance Multi-Element Foil (MEF) Pulp Screen Rotor – Pilot and Mill Trials, Paptac Annual Mtg. Montreal.

HYENSJÖ, M. DAHLKILD A., KROCHAK P., OLSON J., HÄMÄLÄINEN J. (2007), "Modelling the Effect of Shear Flow on Fibre Orientation Anisotropy in a Planar Contraction", Nordic Pulp and Paper Research Journal, vol. 22(3), pp. 376-382.

KEREKES R.J. AND DOUGLAS W.J.M. (1972) "Viscosity properties of suspensions at the limiting

conditions for turbulent drag reduction" Can. J. Chem. Eng, Vol 50 April.

KEREKES R.J. (2006) "Rheology of fibre suspension in papermaking: An Overview of recent research" Nordic Pulp and Paper Research Journal, 21(5) , 598-612

KEREKES, R. AND SCHELL, C., (1992). "Characterization of Fibre Flocculation Regimes by a Crowding Factor", J. Pulp Pap. Sci., 18(1): pp. J32–38

R.J. KEREKES (2009) Personal communication.

KOCH, D.L. 1995 A Model for Orientational Diffusion in Fibre Suspensions Phys. Fluids
7(8) 2086–2088

KROCHAK P., OLSON J.A. AND MARTINEZ M., (2009) "Fiber Suspension Flow in a Tapered Channel: The Effect of Flow/Fiber Coupling" Int. J. Multiphase Flow, Accepted.

MARTINEZ, M., BUCKLEY, K., JIVAN, S., LINDSTRÖM, A., THIRUVENGADASWAMY, R., OLSON, J.A., RUTH, T.J. AND KEREKES, R.J. (2001) "Characterizing the mobility of papermaking fibres during sedimentation", Fundamental Research Symposium, pp. 225-254, Oxford, United Kingdom.

MASON S.G. (1948) "The flocculation of Cellulose Fibre Suspensions", Pulp and Paper Mag. Can. 99-104

OLSON, J.A. AND KEREKES R.J., (1998) "The motion of fibres in turbulent flow," J. Fluid Mech., 377, pp. 47-64

OLSON, J.A., FRIGAARD I., CHAN, C. AND HAMALAINEN, P, (2004) "Modelling a turbulent fibre suspension flowing in a planar contraction: The one-dimensional headbox", Int. J. Multiphase Flow, 30 (1), pp 51-66.

OLSON, J.A., TURCOTTE, S., AND GOODING, R.W., (2004) "Determination of power requirements for solid core pulp screen rotors", Nordic Pulp and Paper Res. J. 19(2):213-217.

POUGATCH SALCUDEAN AND GARTSHORE, (2006) "A numerical model of the reacting multi-phase flow in a pulp digester", Applied Mathematical Modelling 30,pp 209–230.

SIXTA, H. (2006) Handbook of Pulp, Wiley Press

WIKSTROM, AND RASMUSON (1998), "Yield stress of pulp suspensions: The influence of fibre properties and processing conditions", Nordic Pulp Pap. Res. J. 13, 3, 243−250.

